

Article

# Low Delay Inter-Packet Coding in Vehicular Networks

Irina Bocharova <sup>1,2</sup>, Boris Kudryashov <sup>1,2</sup>, Nikita Lyamin <sup>3</sup>, Erik Frick <sup>4</sup>, Maben Rabi <sup>3</sup> and Alexey Vinel <sup>3,5\*</sup>

<sup>1</sup> Department of Information Systems, St.-Petersburg University of Information Technologies, Mechanics and Optics, St.-Petersburg, Russia;

<sup>2</sup> Institute of Computer Science, University of Tartu, Tartu, Estonia;

<sup>3</sup> School of Information Technology, Halmstad University, Halmstad, Sweden;

<sup>4</sup> AstaZero Hällered, Sandhult, Sweden;

<sup>5</sup> Department of Electrical Engineering, Western Norway University of Applied Sciences, Bergen, Norway;

\* Correspondence: alexey.vinel@hh.se; Tel.: +46-35-167984

Version September 29, 2019 submitted to Journal Not Specified

**Abstract:** In Cooperative Intelligent Transportation Systems (C-ITSs), vehicles need to wirelessly connect with Roadside units (RSUs) over limited durations when such point to point connections are possible. One example of such communications is the downloading of maps to the C-ITS vehicles. Another example occurs in the testing of C-ITS vehicles, where the tested vehicles upload trajectory records to the roadside units. Because of real-time requirements, and limited bandwidths, data is sent as User Datagram Protocol (UDP) packets. We propose an inter-packet error control coding scheme that improves the recovery of data when some of these packets are lost; we argue that the coding scheme has to be one of convolutional coding. We measure performance through the session averaged probability of successfully delivering groups of packets. We analyze two classes of convolution codes and propose a low-complexity decoding procedure suitable for network applications. We conclude that Reed-Solomon convolutional codes perform better than Wyner-Ash codes at the cost of higher complexity. We show this by simulation on the memoryless binary erasure channel (BEC) and channels with memory, and through simulations of the IEEE 802.11p DSRC/ITS-G5 network at the C-ITS test track AstaZero.

## 1. Introduction

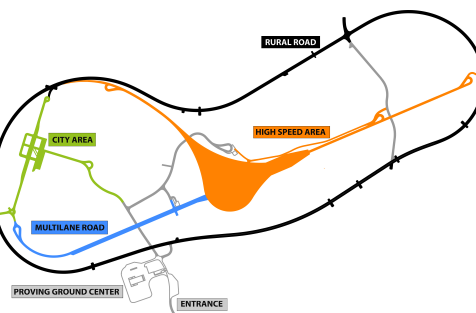
### 1.1. Safety testing of C-ITS

The emerging concept of Cooperative Intelligent Transportation Systems (C-ITS) suggests a widespread adoption of information and communication technologies in diverse vehicular applications that aim at increasing transport safety, efficiency and comfort. C-ITS vehicles exchange information with each other as well as with roadside infrastructure over vehicular ad-hoc networks (VANETs) [1]. An important milestone for VANETs has been the worldwide allocation of reserved bandwidth for C-ITS in the 5.9 GHz spectrum. The developing communication technology is called as DSRC in USA, and ITS-G5 in Europe [2].

Intensive testing is being performed so that C-ITS systems could be introduced on public roads. AstaZero in Sweden is an advanced testbed for research and development in the area of active road safety and autonomous transport [3]. The unique capacities of the testbed offer the opportunity to support and accelerate research and development of active safety and C-ITS features through partnerships and close collaboration with vehicle manufacturers, suppliers, legislators, universities and colleges from throughout the world. Different traffic and communication environments are



(a) Aerial view on the test track



(b) Different test areas

**Figure 1.** Asta-Zero test track.

available at the facility, and these make it possible to test and analyze systems from function level to vehicle integration – and this in all kinds of traffic and traffic situations Fig. 1.

### 1.2. Roadside units and quasi real-time transfers

By leveraging remote connectivity supplied by Road-Side Units (RSUs) deployed along the road in VANETs, vehicles can retrieve/update maps or perform advertisement media downloading [4] via vehicle-to-roadside (V2R) communications. Moreover, vehicles may exploit storage and processing capabilities locally offered by RSUs, according to the recently proposed mobile edge computing (MEC) paradigm [5].

V2R communications are expected to be short-lived and intermittent, due to the high mobility of the vehicles and to the high costs to deploy a ubiquitous roadside infrastructure. Because of the huge data traffic demands of vehicles coupled with the limitations of V2R communications, a practical design must make the best of connectivity opportunities in *drive-thru scenario*, where moving vehicles spend at most a couple of minutes in the coverage area of a RSU [6–8]. When a non-reliable transport protocol is used, an application layer inter-packet coding turns out to be an attractive solution if we aim at transferring as much data as possible.

Drive-through scenario applies to C-ITS vehicular active safety testing also. At the AstaZero testing facility one can test active safety by enacting carefully choreographed scenarios. Each scenario may involve multiple test objects such as vehicles, pedestrians etc. During testing, each test object is fitted with a modem. The purpose is twofold. Firstly the modems send and receive to and from the infrastructure, strictly real-time data consisting of trajectory updates to the test server, scenario abort signals from the test server etc. Secondly the modems upload quasi-real time data consisting of sensor measurements and vehicular log information to the RSUs. In this way some of the data inside the vehicle is available nearly real-time to the RSUs/server for diagnostics in case a vehicle itself ends up damaged. It is this quasi real-time data transfer for which we design inter-packet coding.

**54** 1.3. *Convolutional codes for inter-packet coding*

**55** A specific feature of packets transmission over wireless is that both burst and isolated packet  
**56** losses (erasures) happen. Many papers address this problem (see, for example, [9], [10] and references  
**57** therein). However, low delay and low complexity requirements narrow down the list of coding  
**58** techniques suitable for this application [11]. Moreover, the important feature of drive-thru scenario is a  
**59** short residence time of a vehicle in the coverage area of the RSU. This restriction makes convolutional  
**60** coding practically the only suitable solution to the problem.

**61** Thorough analysis of state-of-art solutions for reliable data transmission in V2V and V2R  
**62** communication scenarios is presented in [12]. Moreover, the batched sparse code (BATS code) [13]  
**63** based protocol is suggested. BATS consists of an outer code and an inner code. The outer code  
**64** represents matrix generalization of the fountain code (see [14]) and the inner code is random linear  
**65** network code. Two studied below classes of convolutional codes can be suggested as low-delay  
**66** alternatives to fountain codes in BATS code construction.

**67** Another specific feature of drive-thru scenario is the existence of entrance and exit zones with  
**68** extremely poor channel conditions which can be characterized by a high probability of communication  
**69** failure. Since error correction coding at physical level cannot improve quality of communication in  
**70** these areas there is a need in packet level error correction. By recovering lost packets at this coding level  
**71** we increase a zone or/and an interval of reliable communication [6–8]. In order to take into account  
**72** nonstationary channel conditions we introduce a new performance measure called successful delivery  
**73** function (SDF). In what follows the studied codes are compared with respect to both conventional  
**74** criteria, such as frame error rate (FER) and bit error rate (BER), and the SDF criterion.

**75** In this paper, we study two classes of high-rate convolutional codes with sliding-window  
**76** (SW)-decoding. The idea to apply convolutional codes to correct packet losses in different networks was  
**77** previously considered in [9,11,15]. We compare the SW-decoding performance of the binary Wyner-Ash  
**78** (WA) convolutional codes [16] and the Reed-Solomon (RS)-convolutional codes [17]. In particular, we  
**79** analyze performances of SW-decoding based on maximum-likelihood (ML) decoding (SWML) and  
**80** belief propagation (BP) decoding (SWBP) of window zero-tail terminated (ZT) convolutional codes  
**81** [18]. A modified low-complexity iterative decoding procedure is suggested. It is shown that extending  
**82** the parity-check matrix of the ZT code by a very limited number of redundant parity-checks (without  
**83** changing the code) leads to the coincidence of the ML and BP decoding performance for this code.

**84** 1.4. *Contributions*

**85** The new contributions of the paper are the following:

- 86** • New low-complexity low-delay decoding algorithm for erasure correction by the Wyner-Ash  
**87** code applied in V2R scenario.
- 88** • Erasure-correcting performance analysis for Wyner-Ash and Reed-Solomon convolutional codes.
- 89** • Comparative analysis of suggested codes and decoding algorithms for (i) memoryless channels,  
**90** (ii) channels with memory described by Gilbert-Elliott model and (iii) real-life VANET provided  
**91** by AstaZero facility.

**92** 1.5. *Organization of the paper*

**93** In Section 2 we formulate the coding problem, and setup a performance measure (1) appropriate  
**94** for short sessions of quasi real-time packet transfers, especially when the channel conditions vary in an  
**95** unknown deterministic way within the session. Two classes of convolutional codes are described and  
**96** analyzed in Section 3. Simulation results are presented and discussed in Section 4. This Section also  
**97** includes the results of calculations based on packet loss measurements from the Asta-Zero test site.  
**98** And finally in Section 5, we indicate future lines of work that naturally emanate from our findings.

**99 2. Preliminaries**

**100 2.1. Wireless channels**

**101** Throughout the paper we assume that at the physical layer data are protected by forward error  
**102** correction. The information packet is organized as a series of codewords and data in the packet are  
**103** protected by cyclic parity check (CRC). The probability of undetected error is negligible. Consequently,  
**104** the decoder after computing CRC classifies each packet either as successfully delivered or as erased.  
**105** Thus, we interpret packet losses as erasures and model packet transmission as a transmission over the  
**106** binary erasure channel (BEC). In this channel either all bits of a packet are successfully received or  
**107** they all are erased. If an erasure correcting code is used, then all encoding and decoding operations  
**108** are performed in parallel with all symbols of the packet. By default, in the coding theory literature it is  
**109** assumed that BEC is a memoryless channel. However, in this paper we consider both memoryless  
**110** BEC and BEC with memory (M-BEC). One example of M-BEC model is obtained from the wireless  
**111** fading channel model by applying discrete model constructing technique in [19,20].

**112 2.2. Performance metric**

**113** Our goal is to improve the reliability of communications by introducing redundancy into the  
**114** transmitted data. When applying this commonly used approach to V2R communications we meet  
**115** specific problems which make it difficult to evaluate the system performance.

**116** First of all, the packet losses cannot be modeled as a random stationary process. For a given  
**117** vehicle and a given RSU we distinguish poor communications zones (entry zone and exit zone) when  
**118** the distance between the receiver and the transmitter is large, and so-called production zone with  
**119** relatively good transmission conditions [7].

**120** As a side effect of non-stationary channel conditions, the conventional criteria such as bit error  
**121** rate (BER) or frame (word, packet) error rate (FER) do not make sense since these quantities change  
**122** over time. The average overall error probability over the session is determined by the worst-case  
**123** values.

**124** In order to formalize the problem of improving reliability of V2R communications we use the  
**125** following approach. Let  $\epsilon_t$  denote the probability of the packet loss at time moment  $t$ , for  $t = 1, \dots, T$   
**126** and where  $T$  is the total number of packets transmitted during one communication session. Assume  
**127** that a message consisting of  $K$  packets should be transmitted, and the transmission is considered as  
**128** successful only if all  $K$  packets are delivered to the receiver. In order to improve reliability,  $N - K$   
**129** redundant packets are added to form a block of length  $N \geq K$  packets, in such a way that if the number  
**130** of lost packets is  $\mu \leq N - K$ , then  $K$  information packets can still be reconstructed by the decoder.  
**131** More precisely, if  $\mu$  is less than the minimum distance of the code then lost packets can always be  
**132** correctly estimated, otherwise, only some of the lost packets can be correctly estimated.

Let  $\xi_t$  denote the indicator function of the successful delivery of the data packet number  $t$  in the  
coded system, with  $t = 1, \dots, T'$ , and where  $T' \leq T$  is the total number of transmitted information  
packets during the session of length  $T$  packets. By definition,  $\xi_t$  is equal to 1 or 0 in case of success or  
failure of delivering packet number  $t$ , respectively. In particular,  $\Pr(\xi_t = 1) = 1 - \epsilon_t$  is the probability  
of successful delivery of the  $t$ th packet. If the message consists of  $K$  packets then the success in  
delivering the entire message can be written in terms of  $\xi_t$  as

$$\left( \sum_{\tau=t}^{t+K-1} \xi_{\tau} \right) = K$$

**133** For a sequence of the  $T'$  transmitted packets the average probability of message delivering should be  
**134** computed as average over  $t = 1, \dots, T' - K + 1$ .

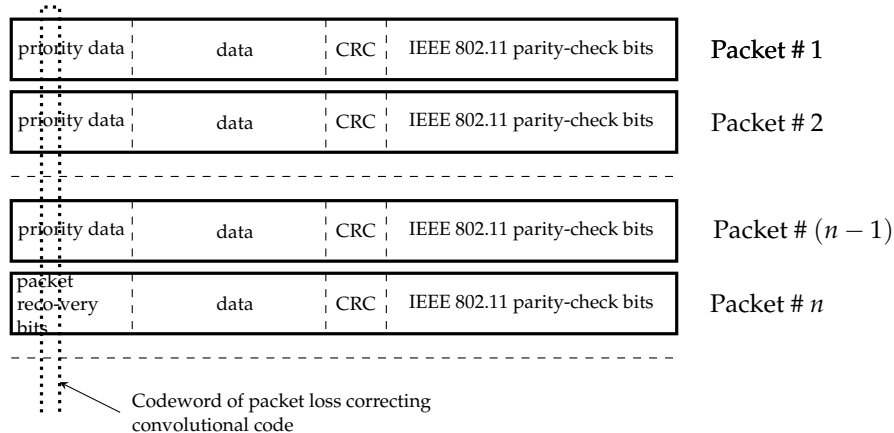


**Figure 2.** Coding for recovering packet losses

The *successful delivery function* (SDF) is defined as

$$P_s(K) \triangleq \frac{1}{T' - K + 1} \sum_{t=1}^{T' - K + 1} \Pr \left\{ \left( \sum_{\tau=t}^{t+K-1} \xi_{\tau} \right) = K \right\}. \quad (1)$$

This function characterizes the average (over session) probability of successful delivery of length  $K$  messages, as a function of  $K$ .

In the particular case of uncoded system, function  $P_s(1)$  equals the fraction of successfully delivered packets, and uncoded transmission is optimal. In general,  $P_s(K)$  decreases as  $K$  grows. This successful delivery function (SDF) shall be our performance measure.

In our analysis we assume that for coverage zones of RSUs the channel parameter  $\epsilon_t$  changes slowly with  $t$  and can be approximated as a constant value for a single block of length  $N$ . This allows us to compare coding systems using different erasure correcting codes by simulating them on the BEC with a fixed symbol erasure probability.

Also, we compare codes using simulation on the M-BEC described by the Gilbert-Elliott model whose parameters do not change during one block of erasure correcting code. For the final evaluation in order to take into account specific of drive-thru scenario we measure SDF by simulation in real-life network conditions.

### 2.3. Convolutional Codes for network applications

Generally speaking, any error-correcting code can be used for recovering lost packets in networks. However, criteria for constructing packet erasure-correcting codes for V2R networks differ significantly from those used for evaluating codes correcting or detecting errors at the physical level. The difference stems from the difference in the acceptable decoding complexity and delay. Short lifetime of the transmitted data makes these requirements much more stronger than for other networks.

Raptor codes [14] represent an efficient low-complexity network-oriented class of codes. However, they are not the best solution for the V2R application since they are meant for correcting large number of independent erasures without restriction on delay, rather than for correcting a small number of erased large packets with strictly limited delay.

Another class of codes which can be efficiently used for recovering packets of erasures are so-called codes with rank metric [21,22]. They were suggested as a generalization of codes for magnetic recording [23]. These codes protect two-dimensional data against both row and column errors and erasures. In the V2R application it is enough to correct one-dimensional erasures which can be equally well done by the Reed-Solomon (RS)-codes [24]. The approach based on convolutional version of the RS-codes [17] is studied below as one of the solutions.

<sup>164</sup> It is well known that complexity of ML decoding over the binary symmetric channel (BSC) and  
<sup>165</sup> over the additive white Gaussian noise (AWGN) channel is, typically, an exponentially growing  
<sup>166</sup> function of code length of block code or of constraint length of convolutional code. For this reason,  
<sup>167</sup> usually codes with simple suboptimal decoding are preferred, e.g. concatenated codes, product codes,  
<sup>168</sup> turbo-codes, LDPC codes, etc.

<sup>169</sup> The situation is completely different for the BEC (M-BEC), where correcting of  $v$  erasures can be  
<sup>170</sup> reduced to solving a system of linear equations of order at most  $v$ . Thus, ML-decoding complexity is a  
<sup>171</sup> polynomial, at most cubic, function of code length. In this case, the decoding delay becomes a basic  
<sup>172</sup> requirement when selecting codes. Convolutional codes, the decoding delay of which is determined by  
<sup>173</sup> the encoder memory and does not depend on the length of the code, have practically no alternative in  
<sup>174</sup> such an application. Low-delay high-rate convolutional codes are among most promising candidates  
<sup>175</sup> for the V2R network application.

<sup>176</sup> The considered further decoding scenario is shown in Fig. 2.

<sup>177</sup> Data packets from the physical layer of the network include data of different priority followed  
<sup>178</sup> by cyclic redundancy check (CRC) and parity-check bits of error detecting code used in IEEE 802.11  
<sup>179</sup> standard. It is assumed that highest priority bits in the sequence of these packets are encoded by a  
<sup>180</sup> convolutional code.

<sup>181</sup> Two classes of binary and nonbinary high-rate convolutional codes are analyzed and compared  
<sup>182</sup> with block codes of the same rate and approximately the same decoding delay. We demonstrate the  
<sup>183</sup> efficiency of these codes when correcting erasures in the BEC and M-BEC obtained from the wireless  
<sup>184</sup> fading channel by using technique in [25]. Then the chosen codes are simulated on the stream of packet  
<sup>185</sup> losses provided by AstaZero.

### <sup>186</sup> 3. Packet recovering codes

<sup>187</sup> In this section, we analyze two solutions, based on low-delay binary and nonbinary convolutional  
<sup>188</sup> codes, respectively. Two low-complexity sliding-window (SW)-decoding procedures are studied. The  
<sup>189</sup> first one is based on ML-decoding applied to the ZT convolutional code inside the window and the  
<sup>190</sup> second implies conventional BP decoding and BP decoding with using redundant parity-check (RPC)  
<sup>191</sup> matrix of the same code [26,27]. As explained below, RPC matrix contains linear dependent rows  
<sup>192</sup> which destroy stopping sets of the code and improve erasure correcting capability compared to BP  
<sup>193</sup> decoding while preserving low decoding complexity.

#### <sup>194</sup> 3.1. Binary Wyner-Ash codes

##### <sup>195</sup> 3.1.1. Code description and distance properties

A binary convolutional code of rate  $R = k/n$  can be characterized by its semi-infinite parity-check matrix

$$H = \begin{pmatrix} H_0 & \mathbf{0} & \cdots & & & & \\ H_1 & H_0 & \mathbf{0} & \cdots & & & \\ H_2 & H_1 & H_0 & \mathbf{0} & \cdots & & \\ \cdots & \cdots & \cdots & \cdots & & & \\ & & & & & & \\ H_m & H_{m-1} & H_{m-2} & H_1 & H_0 & \mathbf{0} & \cdots & \\ \mathbf{0} & H_m & H_{m-1} & \cdots & H_1 & H_0 & \mathbf{0} & \cdots & \\ \cdots & \cdots \end{pmatrix}, \quad (2)$$

<sup>196</sup> where  $m$  denotes the code syndrome memory [18], and for each  $i = 0, 1, \dots, m$ , the entry  $H_i$  is of size  
<sup>197</sup>  $(n - k) \times n$ .

Let us consider one block-column submatrix

$$H^{(m)} = \begin{pmatrix} H_0 \\ H_1 \\ H_2 \\ \vdots \\ H_m \end{pmatrix}. \quad (3)$$

If  $H^m$  is a suitably chosen parity-check matrix of the  $R_b = (n - m - 1)/n$  extended Hamming code of length  $n = 2^m$  with minimum distance  $d_{\min} = 4$ , then (2) determines a subclass of Wyner-Ash codes [16] of rate  $R = (n - 1)/n$  with syndrome memory [18]  $m$  and free distance  $d_{\text{free}} = 3$ .

The subblock codes of the rate  $R = 3/4$  and  $R = 7/8$  Wyner-Ash codes with  $m = 2, 3$ , respectively, are determined by parity-check matrices

$$H^{(2)} = \begin{pmatrix} 1 & 1 & 1 & 1 \\ 1 & 0 & 1 & 0 \\ 1 & 1 & 0 & 0 \end{pmatrix}, \quad (4)$$

$$H^{(3)} = \begin{pmatrix} 1 & 1 & 1 & 1 & 1 & 1 & 1 & 1 \\ 1 & 1 & 1 & 1 & 0 & 0 & 0 & 0 \\ 1 & 1 & 0 & 0 & 1 & 1 & 0 & 0 \\ 1 & 0 & 1 & 0 & 1 & 0 & 1 & 0 \end{pmatrix}. \quad (5)$$

The corresponding polynomial parity-check matrix of the convolutional code for  $m = 2$

$$H(D) = (1 + D + D^2 \ 1 + D^2 \ 1 + D \ 1) \quad (6)$$

has systematic form. Its generator matrix can be written as

$$G(D) = \begin{pmatrix} 1 & 0 & 0 & 1 + D + D^2 \\ 0 & 1 & 0 & 1 + D^2 \\ 0 & 0 & 1 & 1 + D \end{pmatrix}. \quad (7)$$

Generalization to an arbitrary  $m$  is obvious.

Close connection to the Hamming codes allows to compute the exact spectrum of the convolutional code determined by (2) through the known spectra of Hamming codes and their cosets. This analysis was performed in [28]. For example, in case  $m = 2$  the spectrum generating function is

$$g(D) = D^3 \frac{6 + 5D - D^2 - 2D^3 - 3D^4 + 3D^6 - D^7}{1 - 3D - 2D^2 - D^3 + D^5 - D^7}.$$

In Table 1 we present the first 10 coefficients of  $g(D)$  from this paper to further use them for bounding the error probability.

**Table 1.** Weight enumerators for Wyner-Ash codes

$m$	$R$	Spectrum coefficients $g_3, \dots, g_{12}$
2	3/4	6, 23, 80, 290, 1050, 3804, 13782, 49929, 180888, 655334
3	7/8	28, 275, 2456, 22468, 205826, 1885187, 17266158, 158138208, 1448368114, 13265417898
4	15/16	120, 2644, 52456, 1066592, 21738992, 442834486, 9021091078, 183772934474, 3743704654772, 76264411563598

<sup>206</sup> 3.1.2. Encoding

<sup>207</sup> From (7) follows a simple implementation of the systematic encoder. This encoder contains in  
<sup>208</sup> total five delay elements, whereas for the minimal non-systematic encoder only two delay elements  
<sup>209</sup> are required (see [18] for details). However, for the considered application, it is not important since we  
<sup>210</sup> do not use a trellis representation of the code for ML-decoding over the BEC. The decoding complexity  
<sup>211</sup> is at most  $v^3$ , where  $v$  is the number of corrected erasures.

<sup>212</sup> Encoding delay is equal to the encoder block length  $n = 2^m$  since each parity-check bit is computed  
<sup>213</sup> immediately after receiving a new block of  $k = n - 1$  latest information bits.

<sup>214</sup> 3.1.3. Decoding

<sup>215</sup> As mentioned before, we study two decoding algorithms: SW-decoding and its simplified version  
<sup>216</sup> SWBP decoding. A low-complexity modification of SWBP decoding whose error performance tends to  
<sup>217</sup> that of SW-decoding is suggested. First, we reformulate the problem of decoding over the BEC to the  
<sup>218</sup> problem of solving a system of linear equations.

<sup>219</sup> Consider a BEC with erasure probability  $\epsilon$ . Let  $H$  be an  $r_B \times n_B$  parity-check matrix of a binary  
<sup>220</sup>  $(n_B, n_B - r_B)$  block code, with the minimum Hamming distance  $d_{\min}$ . An ML decoder corrects any  
<sup>221</sup> pattern of  $v$  erasures if  $v \leq d_{\min} - 1$ . If  $d_{\min} \leq v \leq r_B$  then a unique correct decision can be obtained  
<sup>222</sup> for some erasure patterns. The number of such correctable patterns depends on the code structure.

<sup>223</sup> Let  $\mathbf{y} = (y_1, y_2, \dots, y_{n_B})$ , be a received vector, where  $y_i \in \{0, 1, \phi\}$ , and the symbol  $\phi$  represents  
<sup>224</sup> an erasure. We denote by  $\mathbf{e} = (e_1, e_2, \dots, e_{n_B})$  a binary vector, such that for all  $i = 1, 2, \dots, n_B$ ,  $e_i = 1$  if  
<sup>225</sup>  $y_i = \phi$ , and  $e_i = 0$  if  $y_i \in \{0, 1\}$ . Let  $I(\mathbf{e})$  be the set of nonzero coordinates of  $\mathbf{e}$ ,  $|I(\mathbf{e})| = v(\mathbf{e})$ , and let  
<sup>226</sup>  $\mathbf{z} = (z_1, z_2, \dots, z_v)$  be a vector of unknowns located in positions of  $I(\mathbf{e})$ .

Consider a system of linear equations  $\mathbf{y}H^T = \mathbf{0}$  which can be reduced to

$$\mathbf{z}H_{I(\mathbf{e})}^T = \mathbf{s}(\mathbf{e}), \quad (8)$$

<sup>227</sup> where the syndrome vector  $\mathbf{s}(\mathbf{e}) = \mathbf{y}_{I^c(\mathbf{e})}H_{I^c(\mathbf{e})}^T$  is computed using the nonerased positions of  $\mathbf{y}$  and  
<sup>228</sup>  $I^c(\mathbf{e}) = \{1, 2, \dots, n_B\} \setminus I(\mathbf{e})$ . ML decoding over the BEC is reduced to solving (8).

<sup>229</sup> Next, we explain SW-decoding of the convolutional code by example of the Wyner-Ash code with  
<sup>230</sup> memory  $m = 2$ .

Let  $L$  denote the decoding delay in blocks. At each step of the decoding procedure, the SW-decoder uses a  $(W - m) \times Wn$  sized parity-check matrix which determines a ZT convolutional code

$$H_{\text{ZT}} = \begin{pmatrix} H_2 & H_1 & H_0 & \mathbf{0} & \cdots \\ \ddots & \ddots & \ddots & \ddots & \ddots \\ \cdots & \mathbf{0} & H_2 & H_1 & \boxed{H_0} & \mathbf{0} & \cdots \\ \cdots & \mathbf{0} & H_2 & \boxed{H_1} & H_0 & \mathbf{0} & \cdots \\ \cdots & \mathbf{0} & H_2 & H_1 & H_0 & \mathbf{0} & \cdots \\ & & & & & \ddots & \ddots \\ & & & & & \cdots & \mathbf{0} & H_2 & H_1 & H_0 \end{pmatrix}, \quad (9)$$

<sup>231</sup> where  $W = L + m + 1$  is the decoding window size in  $n$ -blocks.

Let  $\mathbf{y} = (y_1, y_2, \dots)$  be a semi-infinite input vector of the SW-decoder. Assuming  $m$  first blocks known (for example, all-zero) we start decoding with  $(m + 1)$ st block. The decision is made about  $W - m$  blocks. After decoding (solving the system of linear equations), the recovered symbols are

substituted into input sequence  $\mathbf{y}$ , the decoder outputs the  $(m + 1)$ st block and the window slides by one block. At the  $i$ th step of the decoding procedure the decoder decides about  $\mathbf{y}_W$

$$\mathbf{y}_W = \left( y_{(m+i-1)n} \dots y_{(i-1+W)n} \right)$$

<sup>232</sup> bits and outputs bits  $(y_{(m+i-1)n}, \dots, y_{(m+i)n})$ .

*Example 1:* Let  $L = 2$ . Then a parity-check matrix of the ZT code has the form

$$H_{\text{ZT}} = \begin{pmatrix} 1100 & 1010 & 1111 \\ & 1100 & 1010 & 1111 \\ & & 1100 & 1010 & 1111 \end{pmatrix}. \quad (10)$$

<sup>233</sup> Let  $\mathbf{v} = (110 110 001 000 101 \dots)$  be the information sequence. By using the generator matrix (7) we  
<sup>234</sup> obtain the corresponding codeword  $\mathbf{u} = (1100 1101 0010 0001 1010 \dots)$ . Assume that the received  
<sup>235</sup> sequence is  $\mathbf{y} = (1100 1\phi0\phi 001\phi 0001 1010 \dots)$ .

<sup>236</sup> The SW-decoder starts decoding with the sequence

<sup>237</sup>  $\mathbf{y}_W = (0000 0000 1100 1\phi0\phi 001\phi)$ . The goal is to find codeword bits  $[z_1, z_2, z_3]$  at the erased positions.

**Step 1.** Compute syndrome. The syndrome is equal to  $[0 0 1]$ . From equation (8) follows

$$\begin{pmatrix} 0 & 0 & 0 \\ 1 & 1 & 0 \\ 0 & 0 & 1 \end{pmatrix} \begin{pmatrix} z_1 \\ z_2 \\ z_3 \end{pmatrix} = \begin{pmatrix} 0 \\ 0 \\ 1 \end{pmatrix}.$$

<sup>238</sup> The number of unknowns is larger than the rank of the system which is equal to 2, that is, a  
<sup>239</sup> unique solution does not exist. The decoder outputs only the information part of the first  
<sup>240</sup> erasure-free block  $[1 1 0 0]$ , i.e. output bits at this step are  $[1 1 0]$ .

**Step 2.** Shift the window. Input now is  $\mathbf{y}_W = (0000 1100 1\phi0\phi 001\phi 0001)$ . The syndrome is  
<sup>241</sup> equal to  $[0 0 1]$ . From equation (8) follows

$$\begin{pmatrix} 1 & 1 & 0 \\ 0 & 0 & 1 \\ 1 & 0 & 0 \end{pmatrix} \begin{pmatrix} z_1 \\ z_2 \\ z_3 \end{pmatrix} = \begin{pmatrix} 0 \\ 0 \\ 1 \end{pmatrix}.$$

<sup>242</sup> The unique solution is  $[z_1, z_2, z_3] = [1 1 0]$ . The decoder decision is  $[1 1 0 1]$  and the output is  $[1 1 0]$ .  
<sup>243</sup> At the next step the decoder will recover block  $[0 0 1 0]$  and the output bits are  $[0 0 1]$ .

<sup>244</sup> Notice, that in general, we have to perform Gaussian elimination to solve the system of linear  
<sup>245</sup> equations. However, in our example it was not necessary. The variable  $z_1$  is the only variable of the  
<sup>246</sup> third equation and we found immediately that  $z_1 = 1$ . Similarly, from the second equation we have  
<sup>247</sup>  $z_3 = 0$ . Excluding known variable from the first equation we obtain  $z_2 = 0$ . This algorithm coincides  
<sup>248</sup> with BP decoding used for decoding LDPC codes over the BEC. The formal description of the decoding  
<sup>249</sup> procedure is given below as Algorithm 1. When applying Algorithm 1 to a sliding window, we obtain  
<sup>250</sup> SWBP decoding. Next, we modify the SWBP algorithm in order to increase its erasure-correcting  
<sup>251</sup> capability while keeping its low complexity.

<sup>252</sup> Since the free distance of the convolutional code is  $d_{\text{free}} = 3$ , not every combination of three  
<sup>253</sup> erasures can be corrected by ML decoding. And so, not every combination of three erasures can  
<sup>254</sup> be corrected by the SW or SWBP decoding procedures. When the decoding delay  $L$  grows, the  
<sup>255</sup> performance of SW decoder tends to the performance of the ML decoder. It means that any erasure  
<sup>256</sup> pattern which is not a codeword and does not cover any codeword can be corrected by the SW decoder.

---

**Algorithm 1** BP-BEC

---

**while** there exist parity checks with only one erased symbol **do**  
 Assign to the erased symbol the modulo-2 sum of all  
 nonerased symbols participating in the same parity  
 check.  
**end while**

---

<sup>256</sup> This is not true for SWBP decoding even if  $L$  tends to infinity. An erasure pattern cannot be  
<sup>257</sup> corrected if it is a stopping set or it covers a stopping set [27].

<sup>258</sup> The stopping set is defined as a subset of indices of columns in its parity-check matrix, such that a  
<sup>259</sup> matrix constructed from these columns does not have a row of weight one. The size of the smallest  
<sup>260</sup> stopping set is called stopping distance  $d_{\text{stop}}$ .

Although, in general,  $d_{\text{stop}} \leq d_{\min}$ , for the Wyner-Ash convolutional code  $d_{\text{stop}} = d_{\text{free}}$ . However,  
 there are many combinations of weight 3 which are not codewords but are stopping sets. For example,  
 consider the column block

$$\begin{pmatrix} H_0 \\ H_1 \\ H_2 \\ \vdots \end{pmatrix} = \begin{pmatrix} 1 & 1 & 1 \\ 1 & 0 & 1 \\ 1 & 1 & 0 \\ 0 & 0 & 0 \\ \dots & \dots & \dots \end{pmatrix}$$

<sup>261</sup> The corresponding positions of the codeword form a stopping set.

<sup>262</sup> Notice, that spectrum of stopping sets is determined not by code, but by its parity-check matrix.  
<sup>263</sup> We can modify a parity-check matrix to eliminate some stopping sets, and thereby make performance  
<sup>264</sup> of BP decoding close to that of ML decoding (see [27,29]). In order to do this, an additional (redundant)  
<sup>265</sup> parity-check should be added to the code parity-check matrix.

For each window we suggest to use the extended parity-check matrix

$$H_{\text{EZT}} = \begin{pmatrix} 1100 & 1010 & 1111 & & \\ & 1100 & 1010 & 1111 & \\ & & 1100 & 1010 & 1111 \\ 1100 & 0110 & 1001 & 0101 & 1111 \end{pmatrix} \quad (11)$$

<sup>266</sup> instead of (10). The additional row is obtained as modulo 2 sum of all previous rows. It is easy to see  
<sup>267</sup> that the former stopping set consisting of positions 9–11 (as well as many others) is not a stopping set  
<sup>268</sup> for this matrix.

<sup>269</sup> The efficiency of the decoding technique based on using the redundant parity-check (RPC) matrix  
<sup>270</sup> will be demonstrated in Section 4.

<sup>271</sup> *3.2. Nonbinary convolutional codes*

<sup>272</sup> *3.2.1. Code description and error-correcting properties*

<sup>273</sup> The advantage of the binary Wyner-Ash codes is high efficiency under very short decoding delay  
<sup>274</sup> and extremely simple decoding algorithm.

<sup>275</sup> Error-correcting properties can be further improved at the cost of additional decoding complexity  
<sup>276</sup> if instead of binary digits we consider  $c$ -tuples of bits or even entire packets as message symbols.

<sup>277</sup> The corresponding convolutional code will be a code over the Galois field extension  $\text{GF}(2^c)$ .  
<sup>278</sup> Generalization of the Wyner-Ash construction to non-binary alphabets for correcting independent  
<sup>279</sup> errors and error bursts was presented in [17], where these codes are called “Reed-Solomon (RS)  
<sup>280</sup> convolutional codes”. Here we analyze efficiency of these codes when used for correcting erasures or  
<sup>281</sup> recovering lost packets in the network.

For simplicity, we consider rate  $R = (n - 1)/n$  codes with memory  $m = 2$ . A semi-infinite parity-check matrix of the code has the form (2), where the main submatrix (3) is equal to

$$H^{(m)} = \begin{pmatrix} H_0 \\ H_1 \\ H_2 \end{pmatrix} = \begin{pmatrix} 1 & 1 & \cdots & 1 \\ 1 & \alpha & \cdots & \alpha^{n-1} \\ 1 & \alpha^2 & \cdots & \alpha^{2(n-1)} \end{pmatrix} \quad (12)$$

and  $\alpha$  denotes a primitive element of the field  $GF(2^c)$ .

*Theorem 1:* If the parity-check matrix of  $R = (n - 1)/n$ ,  $n \geq 4$  convolutional code over  $GF(2^c)$ ,  $c > \log_2 n$ , is defined by (2) with submatrices defined by (12) then free distance of the convolutional code is  $d_{\text{free}} = 4$ .

**Proof.** Let  $\nu = (\nu_1, \nu_2, \dots)$  denote a sequence of numbers of the erased positions on the 1st, 2nd, ... subblocks of length  $n$ . It is enough to prove that any erasure pattern such that

$$\sum_{i=1}^{\infty} \nu_i \leq 3$$

will be recovered using SW decoding, and there exists an uncorrectable erasure pattern of weight 4. In order to prove the negative statement, consider the sequence  $\nu = (4, 0, 0, \dots)$ . Three parity checks of the matrix (12) will contain 4 unknown variables and, therefore, a unique decision does not exist.

In order to prove that all erasure patterns of 3 or less erasures will be corrected we show that the following two statements are true:

1. Any erasure pattern  $\nu = (\nu_1, \nu_2, \dots, \nu_N)$  such that  $\nu_1 \leq 3$  and  $\nu_i = 0$ ,  $i \neq 1$  for any  $N$  will be corrected.
2. Any erasure pattern  $\nu = (\nu_1, \nu_2, \dots, \nu_N)$  such that  $\nu_1 < 3$ ,  $\sum_i \nu_i = 3$  will be corrected.

The first property follows from the fact that the corresponding subblock codes are the RS-codes of length  $n \geq 4$  and  $d_{\min} = 4$ . The second property follows from the fact that any three columns belonging to different subblocks are linearly independent if  $c > \log_2 n$  and the Vandermonde matrix (12) is non-degenerate [24].

In other words, for the worst case  $\nu = (2, 1, 0, \dots)$  the corresponding columns of the parity-check matrix have the form

$$\begin{pmatrix} 1 & 1 & 0 \\ \alpha^i & \alpha^j & 1 \\ \alpha^{2i} & \alpha^{2j} & \alpha^h \\ 0 & 0 & \alpha^{2h} \end{pmatrix}$$

where  $i < j < n$ ,  $h < n$ . These columns are linearly independent, therefore, correction of such erasure pattern is guaranteed.  $\square$

We already proved that uncorrectable erasure patterns of weight four having their ones in one subblock cannot be corrected. In what follows, we show that if four erasures are located in different subblocks then such erasure patterns can always be corrected.

*Theorem 2:* If the parity-check matrix of  $R = (n - 1)/n$ ,  $n \geq 4$  convolutional code over  $GF(2^c)$ ,  $c > 2n$ , is defined by (2) with submatrices defined by (12) then all erasure patterns of weight four except for the  $\binom{n}{4}$  erasure patterns can be corrected.

**Proof.** According to property 1 of Theorem 1 all correctable erasure patterns of weight four having their ones in one block cannot be corrected. Thus, there are  $\binom{n}{4}$  uncorrectable erasure patterns.

Now consider erasure patterns of weight four whose erasures are located in different subblocks. According to the listed above code properties only combination  $\nu = (2, 2, 0, 0, \dots)$  requires an additional

analysis. The corresponding equations with respect to the unknowns  $(z_1, z_2, z_3, z_4)$  are determined by the parity-check matrix

$$\begin{pmatrix} 1 & 1 & 0 & 0 \\ \alpha^i & \alpha^{i'} & 1 & 1 \\ \alpha^{2i} & \alpha^{2i'} & \alpha^j & \alpha^{j'} \\ 0 & 0 & \alpha^{2j} & \alpha^{2j'} \end{pmatrix} \quad (13)$$

The determinant of (13) is

$$\Delta = (\alpha^i + \alpha^{i'})(\alpha^j + \alpha^{j'})(\alpha^i + \alpha^{i'} + \alpha^{j+j'})$$

The equality  $\Delta = 0$  is equivalent to the equality

$$\alpha^i + \alpha^{i'} + \alpha^{j+j'} = 0, \quad (14)$$

and never happens if  $c > 2n$  since  $\alpha^{j+j'}, j + j' < 2n < c$  is a basis field element and, consequently, it has binary representation of Hamming weight 1. Then the Hamming weight of the binary representation of the LHS of (14) is equal either to 1 or to 3. Therefore determinant of the system is nonzero and there are no nontrivial solutions of weight less or equal to four.  $\square$

More detailed analysis for the case  $n = 4$  allows to compute the generating function of weights of unrecoverable erasure patterns as a function of formal variable  $D$

$$f(D) = \frac{a(D)}{b(D)},$$

where  $a(D)$  and  $b(D)$  are polynomials of degree 20 and 16, respectively. Probability of packet loss after decoding can be expressed via  $f(D)$  as follows

$$P_e = \frac{1}{n} f(D)|_{D=\epsilon}, \quad (15)$$

where  $\epsilon$  is the channel erasure probability. The series expansion of (15) is

$$P_e = \frac{1}{n} \sum_{i=d_{\text{free}}}^{\infty} f_i \epsilon^i, \quad (16)$$

where  $f_i$  denotes the  $i$ th coefficient in series expansion of  $f(D)$ , that is, the number of uncorrectable erasure patterns of weight  $i$ . It was found numerically that for  $\epsilon \leq 1/4$  the first 8 coefficients are enough to compute  $P_e$  with high precision. The first coefficients  $f_i$  in (16) are given in Table 2.

**Table 2.** Coefficients of series expansion of  $f(D)$  for the RS convolutional code of rate  $R = 3/4$

$m$	$R$	Series expansion coefficients $f_4, \dots, f_{11}$
2	3/4	1, 32, 342, 2282, 8756, 9657, -102562, -773838

In what follows, (16) which does not take into account the decoding delay and computed with coefficients from Table 2 is interpreted as the lower bound on the packet loss probability for the RS convolutional codes on the BEC.

### 3.2.2. Encoding and decoding for the RS-convolutional codes

We do not obtain a generator matrix of the RS-convolutional code. Instead we construct a codeword in the systematic form calculating a single parity-check symbol of each subblock recursively.

A semi-infinite parity-check matrix of the RS-convolutional code is defined by (2) and (12). The encoding procedure can be simplified by rewriting columns of  $H^{(m)}$  in (12) in the reverse order. In particular, for  $R = 3/4$  and  $n = 4$  the reordered matrix has the form

$$H^{(m)} = \begin{pmatrix} H_0 \\ H_1 \\ H_2 \end{pmatrix} = \begin{pmatrix} 1 & 1 & 1 & 1 \\ \alpha^3 & \alpha^2 & \alpha & 1 \\ \alpha^6 & \alpha^4 & \alpha^2 & 1 \end{pmatrix} \quad (17)$$

Denote by

$$\tilde{H} = \begin{pmatrix} 1 & 1 & 1 \\ \alpha^3 & \alpha^2 & \alpha \\ \alpha^6 & \alpha^4 & \alpha^2 \end{pmatrix}$$

the information part of  $H^{(m)}$ . The codeword of the RS-convolutional code over  $\text{GF}(2^c)$  can be written in the form  $\mathbf{u}_1, v_1, \mathbf{u}_2, v_2, \dots$  where  $\mathbf{u}_i = (u_{i1}, u_{i2}, u_{i3})$  are message blocks consisting of three information symbols from  $\text{GF}(2^c)$  and  $v_i$  are the corresponding parity-check symbols. Denote by  $\mathbf{s}_i = (s_{i1}, s_{i2}, s_{i3}) = \mathbf{u}_i \tilde{H}^T$  a partial syndrome computed for the information block. It is easy to see that the first check symbol  $v_1 = s_{11}$  and the next one depends on  $s_{12}$ , etc. The following recurrent equations describe encoding for the RS-convolutional code.

$$\begin{aligned} v_1 &= s_{1,1}, v_2 = v_1 + s_{1,2} + s_{2,1}, \\ v_i &= v_{i-2} + v_{i-1} + s_{i-2,3} + s_{i-1,2} + s_{i,1}, i = 3, 4, \dots \end{aligned} \quad (18)$$

- <sup>321</sup> Notice that if the field extension parameter  $c > n$  then all elements of parity-check matrix (12) have the  
<sup>322</sup> Hamming weight 1 and all multiplications in (18) are implemented as simple cyclic shifts.  
<sup>323</sup> For the RS-convolutional codes SWML-decoding is implemented similarly to that for the binary  
<sup>324</sup> WA codes. The difference is that the parity-check matrix is more dense (does not contain zeros on  
<sup>325</sup> non-trivial positions) and arithmetic operations are performed over the field  $\text{GF}(2^c)$ .

#### <sup>326</sup> 4. Numerical results

<sup>327</sup> In this section we compare codes and coding techniques described in Section 3. Only  $R = 3/4$   
<sup>328</sup> codes with syndrome memory  $m = 2$  are studied since they provide the smallest delay and lowest  
<sup>329</sup> complexity requirements. First, in subsection 4.1 we consider a memoryless channel (BEC) and study  
<sup>330</sup> influence of the code and decoder parameters on the packet-recovering performance. In subsection 4.2  
<sup>331</sup> we investigate performance of the Wyner-Ash and the RS-convolutional codes in the channel with  
<sup>332</sup> memory (M-BEC) where packet losses are generated according to the Gilber-Elliott model obtained  
<sup>333</sup> from the fading channel model as explained in [19,20].

##### <sup>334</sup> 4.1. Memoryless channel (BEC)

<sup>335</sup> As a channel model we consider the BEC with erasure (packet loss) probability  $\epsilon$ .

<sup>336</sup> In Fig. 3 we compare the probability of packet loss after decoding the Wyner-Ash code by using  
<sup>337</sup> two decoding methods: the maximum-likelihood SW-decoder (SWML decoder) with delay  $L = 4$  and  
<sup>338</sup> subblock length  $n = 4$  and the SWBP-decoder with one redundant parity check (SWBP-RPC decoding)  
<sup>339</sup> with delays  $L = 2, 3, 4$ . We do not show the SWML decoding performance for  $L = 2$  and 3 since the  
<sup>340</sup> corresponding plots differ negligibly from the plot for  $L = 4$ .

Also we present a lower bound on the decoding performance without restrictions on the decoding delay. This bound is obtained from the spectrum of the Wyner-Ash code presented in Table 1. Only the first term is taken into account, and this gives:

$$P_e \geq 18\epsilon^3 / 4. \quad (19)$$

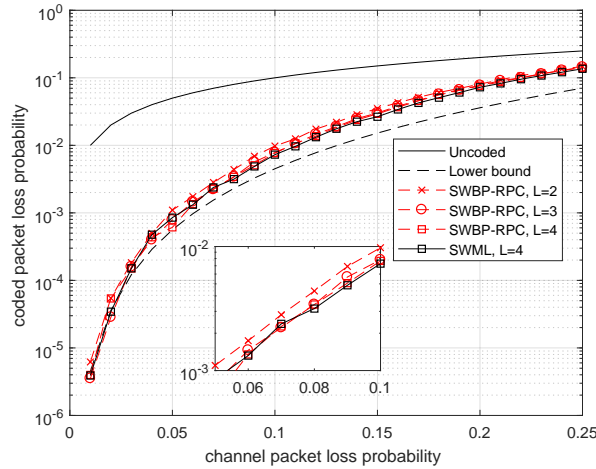


**Figure 3.** Comparison of SWML decoding and SWBP decoding with RPC of the binary Wyner-Ash code of rate  $R = 3/4$

341 The plots shown in Fig. 3 demonstrate that both SWBP-RPC and SWML decoding provide the packet  
 342 recovering performance rather close to the lower bound. Therefore, the delay value  $L = 4$  is enough  
 343 for achieving near optimum performance almost in the entire range of packet loss rates  $\epsilon$ . Also we  
 344 noticed that the decoding performance is not critical with respect to the decoding delay and  $L = 2$  is  
 345 an acceptable value. Moreover, a very simple SWBP-RPC decoder performs almost as good as more  
 346 complicated (yet simple) SWML decoder requiring Gaussian elimination for correcting erasures.

347 In Fig. 4 we analyze the coding gain from using SWBP-RPC decoding compared to SWBP  
 348 decoding. We chose decoding delay  $L = 2$  since it follows from the previous plot that increasing  
 349 delay does not improve the performance significantly. We conclude from this plot that even the SWBP  
 350 decoder works very well. However, it is worth using the SWBP-RPC decoder because of an additional  
 351 gain in performance which can be obtained at the cost of negligible increase in decoding complexity.

352 In Fig. 5 binary and nonbinary (RS) convolutional coding efficiency is compared. Surprisingly,  
 353 when the decoding delay is small,  $L = 2$ , the two codes have near the same efficiency. However,  
 354 if the allowed decoding delay grows, the RS convolutional codes become more efficient. We also  
 355 compare the packet loss probability with the lower bound (16) achievable without restriction on the  
 356 decoding delay. Again, we can see that the SWML-decoder for the RS convolutional code achieves  
 357 near optimal performance already for  $L = 4$ . Notice that if  $L$  grows then the decoding complexity  
 358 grows approximately proportional to  $L^3$ .

359 It is interesting to compare efficiency of the considered convolutional codes to block codes under  
 360 the same delay constraints. Delay  $L = 2$  and 4 correspond to the length of block codes  $N = 12$  and 20,  
 361 respectively. The block codes of rate  $R_b = 3/4$  with the best minimum distance for given length and  
 362 rate were chosen for comparison.

363 In Fig. 6 the comparison is done for binary codes. The convolutional code with delay  $L = 2$   
 364 provides almost the same efficiency as the block code with code length  $N = 20$ . Moreover, typically,  
 365 if one erasure occurs then the SWML-decoder outputs the result with delay at most 4, whereas the  
 366 decoder of block code processes the entire codeword of length 20.

367 In Fig. 7 we can see that the relation between nonbinary RS-block and RS-convolutional codes  
 368 differs from that for binary codes. The RS-block code of length 12 loses very little compared to the  
 369 RS-convolutional code. With increasing delay the advantage of convolutional codes increases. Notice  
 370 that the decoding complexity for the convolutional code is less than that for the block codes since its  
 371 parity-check matrix is more sparse.

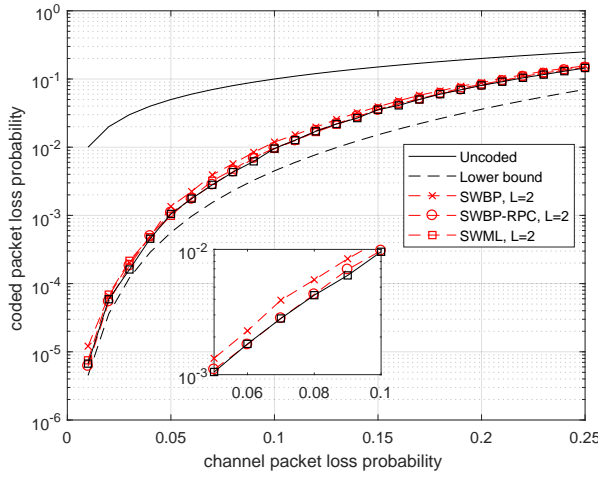


**Figure 4.** Comparison of SWBP, SWBP-RPC and SWML decoding of the binary Wyner-Ash code of rate  $R = 3/4$

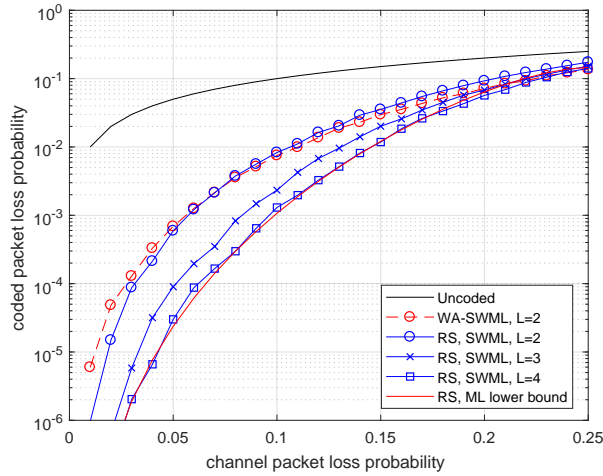


**Figure 5.** Comparison of the binary Wyner-Ash code and the RS convolutional code of rate  $R = 3/4$

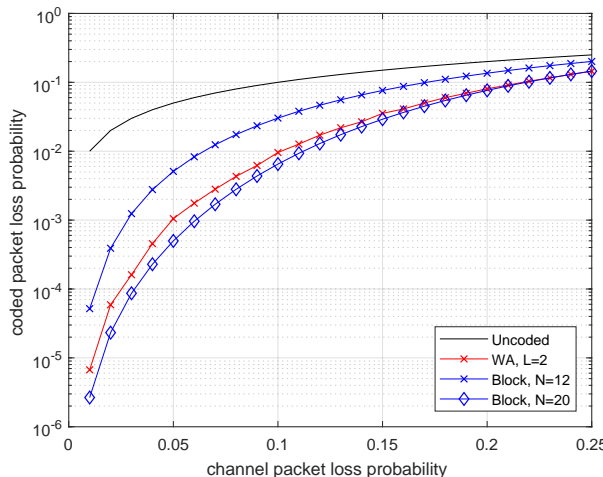


**Figure 6.** Comparison of rate 3/4 block codes and the WA convolutional code for different decoding delays

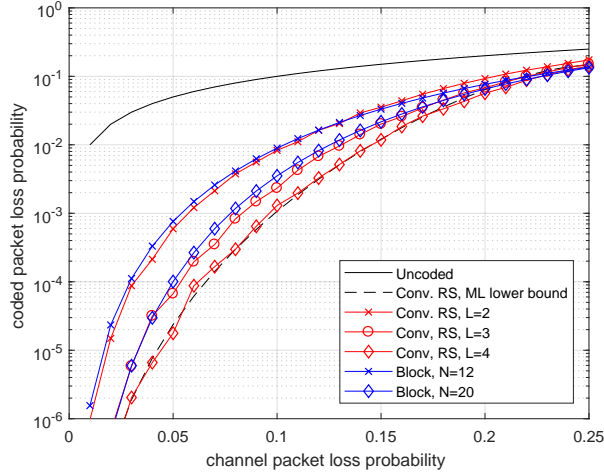


**Figure 7.** Comparison of RS-block codes and the RS-convolutional code for different delays

#### 372 4.2. Channel with memory (M-BEC)

373 In this subsection we compare performance of the binary WA codes and the RS-convolutional  
 374 codes on the erasure channel with memory. We model this channel as a discrete approximation of the  
 375 fading channel. The Rice fading channel model is determined by signal-to-noise ratio  $E/N_0$ , correlation  
 376 coefficient  $\rho$  and coefficient  $k^2$  characterizing ratio of energies of regular and random components of  
 377 the received signal. If  $k = 0$  we obtain the Rayleigh fading channel. We approximate this channel by  
 378 the Gilbert-Elliott model using technique in [19,20]. See also tutorial [30] for overview of approaches  
 379 to constructing finite-state discrete approximations of analog wireless channel models.

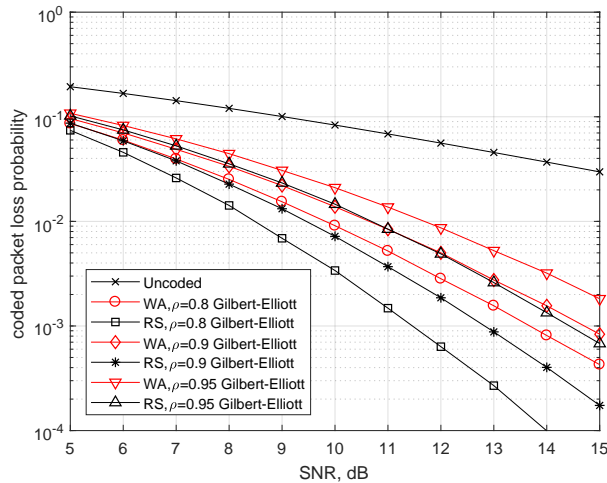


**Figure 8.** Comparison of the binary rate  $R = 3/4$  WA code with the rate  $R = 3/4$  RS-convolutional code for different correlation coefficients of the fading channel

380 In Fig. 8 the same codes with SWML-decoding are compared over the Gilbert-Elliott model  
 381 approximating the Rayleigh fading with  $\rho = 0.8$ ,  $\rho = 0.9$ , and  $\rho = 0.95$  [25], [19]. The decoding  
 382 performance rapidly degrades with increasing correlation coefficient. Larger delay codes are superior  
 383 with respect to the codes with  $L = 2$ . The obtained coding gain decreases from 2 dB to 1 dB with  
 384 increasing  $\rho$  from 0.8 to 0.95, respectively.

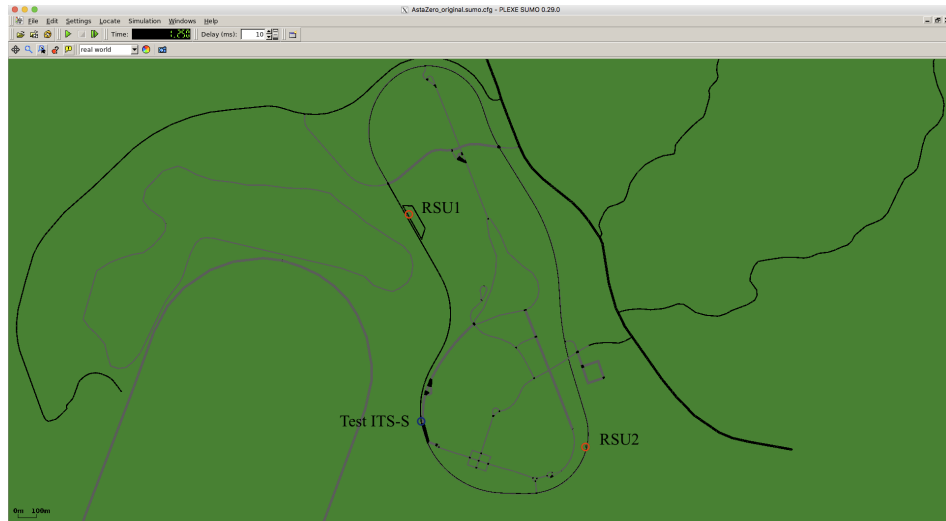


**Figure 9.** AstaZero test area in simulation environment

**385 4.3. Probability of message successful delivering for AstaZero scenario**

**386** In Fig. 9 the general view of the rural test area of AstaZero is shown. We consider two RSUs that  
**387** are placed such that, together they cover most of the test track.

**388** Simulation parameters for Fig. 10 are as follows: transmission power 200 mW (23 dBm - maximum  
**389** allowed power on control ITS-G5 channel), datarate 6 Mbit/s, packet size 400 Bytes, ITS-s generates  
**390** 1500 msg/s,  $m = 1$  in the Nakagami-m model, simulation time - 425 seconds (time for one full circuit  
**391** drive on the test track with the constant speed of 50 km/h), the code rate  $R = 3/4$ . In Fig. 10 blue  
**392** circles demonstrate the packets received before decoding, and red crosses depict packets additionally  
**393** recovered by the decoder<sup>1</sup>. Predictably, the demonstrated performance is best next to each RSU,  
**394** when ITS-s resides in the production zone. Here we present the simulated probability of successful  
**395** delivering  $P_s(K)$  (SDF) determined by equation (1) as a function of message length  $K$ . The WA and  
**396** RS convolutional codes under SWML decoding are considered. In Figs. 11 and 12 we show the SDFs  
**397** for the WA binary convolutional codes used over the production zone and over the entire session,  
**398** respectively. In Figs. 11, 12, the SDFs obtained for different code rates and for uncoded transmission  
**399** are compared. As follows from the presented plots, the lower code rate, the better reliability of packet  
**400** delivering can be achieved. However, it seems that decreasing the code rate below  $R = 7/8$  does not  
**401** lead to a significant improvement and this rate can be considered as a reasonable choice. During the  
**402** production zone successful delivering of message of length up to 1000 packets is highly probable. For  
**403** the entire session only about 10% of long messages will be delivered even for the coded system.

**404** In Figs. 13 and 14, we compare the WA codes versus the RS codes for the production zone and  
**405** for the entire session, respectively. We conclude that the RS codes provide better reliability of the  
**406** transmission compared to the WA codes but at the cost of higher computational complexity.

**407** Both classes of codes demonstrate high reliability of delivering long message during the  
**408** production zone.

**409 5. Conclusions**

**410** In summary, we have shown that significant gains come through our proposed erasure codes.  
**411** From the figures of the previous section, it is clear that there is a significant difference in the probability  
**412** of successful delivery, between codes and uncoded transmissions. Our new algorithm has low delay  
**413** and low complexity, and is based on Wyner-Ash convolutional codes. We conducted an erasure

<sup>1</sup> For representational purposes all the points for recovered packets were moved 20 m to the left.

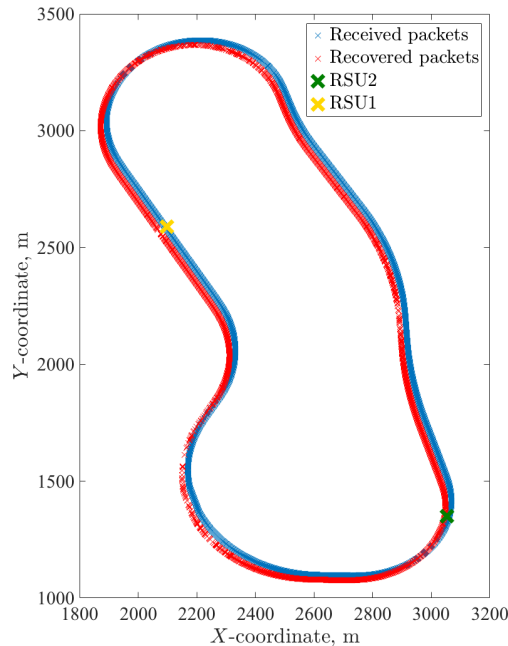


**Figure 10.** AstaZero scenario results

414 performance analysis for both these Wyner-Ash convolutional codes, and also for corresponding  
 415 ones based on Reed-Solomon convolutional codes. Thus our main recommendation for V2R  
 416 communications is to apply erasure codes for boosting packet reception rates.

417 Our future work towards the support of C-ITS safety testing is planned in three main directions.

418 First is the experimental proof-of-concept validation of the developed inter-packet coding scheme,  
 419 to be performed at AstaZero.

420 Secondly, we are planning to propose such inter-packet coding in the ongoing ISO 22133-1  
 421 standardization of messages formats and communication protocols for automotive testing facilities.

422 Finally, we intend to address tighter requirements on decoding delays. The studied coding scheme  
 423 introduces some delays which are acceptable for non-critical (quasi real-time) VANET scenarios like  
 424 maps updates, but these delays are not acceptable for hard real-time data traffic (e.g. the tracking of  
 425 objects under test). Therefore, designing of appropriate coding schemes which meet the reliability  
 426 requirements for hard real-time C-ITS applications will be a subject of our future work.

## 427 Acknowledgements

428 The research leading to the results reported in this work has received funding from the Knowledge  
 429 Foundation in the framework of AstaMoCA "Model-based Communication Architecture for the  
 430 AstaZero Automotive Safety" project (2017–2019), COST Action CA15127 ("Resilient communication  
 431 services protecting end-user applications from disaster-based failures – RECODIS") supported by  
 432 COST (European Cooperation in Science and Technology), Swedish Foundation for Strategic Research  
 433 (SSF) in the framework of Strategic Mobility Program (2019–2020), from the Estonian Research Council  
 434 under the grant PRG49 and from the ELLIIT Strategic Research Network. This support is gratefully  
 435 acknowledged.

436

- 437 1. Zheng, K.; Zheng, Q.; Chatzimisios, P.; Xiang, W.; Zhou, Y. Heterogeneous Vehicular Networking: A Survey  
 438 on Architecture, Challenges, and Solutions. *IEEE Communications Surveys Tutorials* **2015**, *17*, 2377–2396.

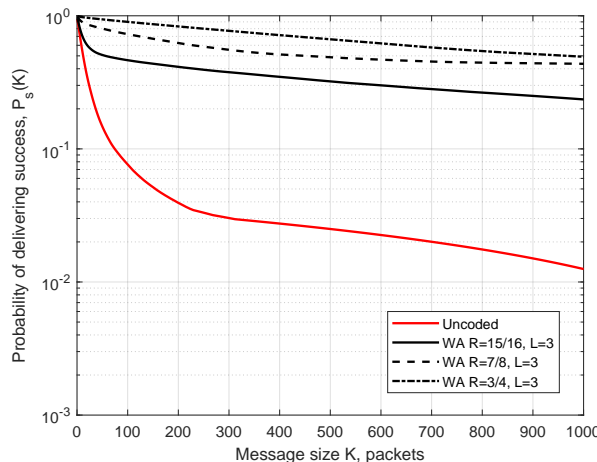


**Figure 11.** SDF for the production zone. Simulation results for the WA codes of different rates used over production zone

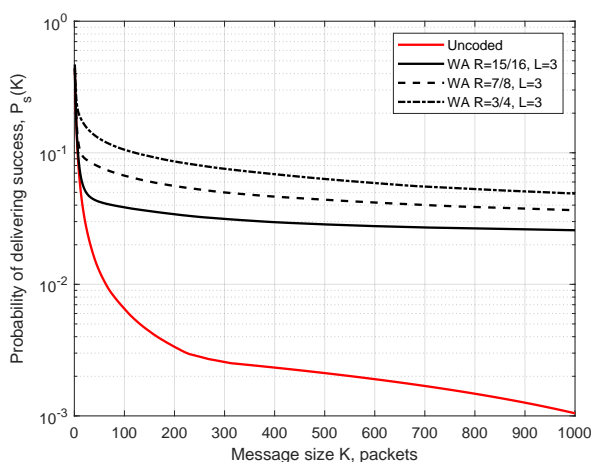


**Figure 12.** SDF for the entire session. Simulation results for the WA codes of different rates used over the entire session

- 439 2. Sjoberg, K.; Andres, P.; Buburuzan, T.; Brakemeier, A. Cooperative Intelligent Transport Systems in Europe:  
440 Current Deployment Status and Outlook. *IEEE Vehicular Technology Magazine* **2017**, *12*, 89–97.
- 441 3. AstaZero Test Site. url = <http://www.astazero.com/the-test-site/test-environments/>.
- 442 4. ETSI. Intelligent Transport Systems (ITS); Vehicular Communications; Basic Set of Applications; Definitions.  
*ETSI TS 102 638 V1.1.1 (2009-06)* **2014**.
- 443 5. Zhang, K.; Mao, Y.; Leng, S.; Maharjan, S.; Vinel, A.; Zhang, Y. Contract-theoretic Approach for Delay  
444 Constrained Offloading in Vehicular Edge Computing Networks. *ACM/Springer Mobile Networks and*  
445 *Applications (MONET)* **2018**, pp. 1–12.
- 446 6. Xing, M.; He, J.; Cai, L. Maximum-Utility Scheduling for Multimedia Transmission in Drive-Thru Internet.  
447 *IEEE Transactions on Vehicular Technology* **2016**, *65*, 2649–2658.
- 448 7. Zhou, H.; Liu, B.; Hou, F.; Luan, T.H.; Zhang, N.; Gui, L.; Yu, Q.; Shen, X.S. Spatial Coordinated Medium  
449 Sharing: Optimal Access Control Management in Drive-Thru Internet. *IEEE Transactions on Intelligent*  
450 *Transportation Systems* **2015**, *16*, 2673–2686.
- 451 8. Atallah, R.F.; Khabbaz, M.J.; Assi, C.M. Modeling and Performance Analysis of Medium Access Control  
452 Schemes for Drive-Thru Internet Access Provisioning Systems. *IEEE Transactions on Intelligent Transportation*  
453 *Systems* **2015**, *16*, 3238–3248.
- 454 9. Martinian, E.; Sundberg, C.E. Burst erasure correction codes with low decoding delay. *IEEE Trans. Inform.*  
455 *Theory* **2004**, *50*, 2494–2502.

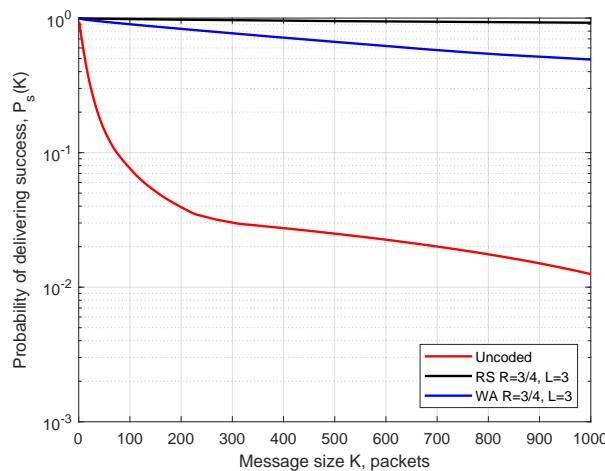


**Figure 13.** SDF for the production zone. Comparison of the WA and the RS codes of rate  $R = 3/4$

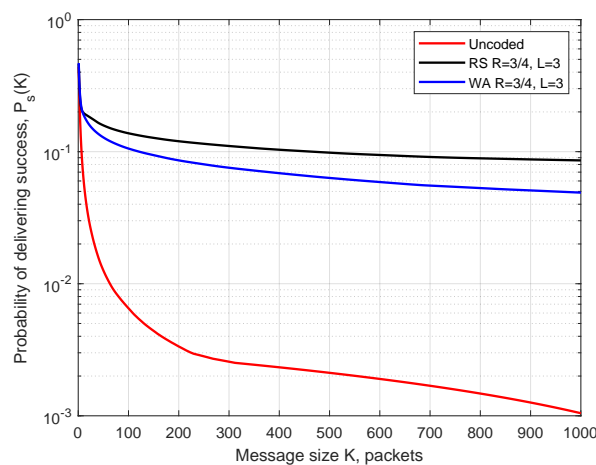


**Figure 14.** SDF for the entire session. Comparison of the WA and the RS codes of rate  $R = 3/4$

- 457 10. Johnson, S.J. Burst erasure correcting LDPC codes. *IEEE Trans. Comm.* **2009**, *57*, 641–652.  
 458 11. Badr, A.; Khisti, A.; Tan, W.T.; Apostolopoulos, J. Streaming codes for channels with burst and isolated  
 459 erasures. INFOCOM, 2013 Proceedings IEEE, 2013, pp. 2850–2858.  
 460 12. Gao, Y.; Xu, X.; Guan, Y.L.; Chong, P.H.J. V2X content distribution based on batched network coding with  
 461 distributed scheduling. *IEEE Access* **2018**, *6*, 59449–59461.  
 462 13. Yang, S.; Yeung, R.W. Batched sparse codes. *IEEE Transactions on Information Theory* **2014**, *60*, 5322–5346.  
 463 14. Shokrollahi, A.; Luby, M.; et al.. Raptor codes. *Foundations and Trends in Communications and Information  
 464 Theory* **2011**, *6*, 213–322.  
 465 15. Arai, M.; Yamaguchi, A.; Fukumoto, S.; Iwasaki, K. Method to recover lost Internet packets using  $(n, k, m)$   
 466 convolutional codes. *Electronics and Communications in Japan (Part III: Fundamental Electronic Science)* **2005**,  
 467 *88*, 1–13.  
 468 16. Wyner, A.; Ash, R. Analysis of recurrent codes. *IEEE Trans. Inform. Theory* **1963**, *9*, 143–156.  
 469 17. Ebert, P.; Tong, S. Convolutional Reed-Solomon Codes. *Bell Labs Technical Journal* **1969**, *48*, 729–742.  
 470 18. Johannesson, R.; Zigangirov, K.S. *Fundamentals of convolutional coding*; John Wiley & Sons, 2015.  
 471 19. Bocharova, I.; Kudryashov, B.; Rabi, M.; Lyamin, N.; Dankers, W.; Frick, E.; Vinel, A. Modeling packet  
 472 losses in communication networks. IEEE International Symposium on Information Theory (ISIT), 2019, pp.  
 473 1–5.  
 474 20. Bocharova, I.; Kudryashov, B.; Rabi, M.; Lyamin, N.; Dankers, W.; Frick, E.; Vinel, A. Characterizing Packet  
 475 Losses in Vehicular Networks. *IEEE Transactions on Vehicular Technology* **2019**, *in press*.

- 476 21. Gabidulin, E.M. Theory of codes with maximum rank distance. *Problemy Peredachi Informatsii* **1985**, 21, 3–16.
- 477 22. Roth, R.M. Maximum-rank array codes and their application to crisscross error correction. *IEEE Trans. Inform. Theory* **1991**, 37, 328–336.
- 478 23. Blaum, M.; McEliece, R. Coding protection for magnetic tapes: A generalization of the Patel-Hong code. *IEEE Trans. Inform. Theory* **1985**, 31, 690–693.
- 479 24. MacWilliams, F.J.; Sloane, N.J.A. *The theory of error-correcting codes*; Elsevier, 1977.
- 480 25. Bocharova, I.E.; Kudryashov, B.D. Development of Discrete Models for Fading Channels. *Problemy Peredachi Informatsii* **1993**, 29, 58–67.
- 481 26. Yakimenka, Y.; Skachek, V.; Bocharova, I.E.; Kudryashov, B.D. Stopping redundancy hierarchy beyond the minimum distance. *IEEE Trans. Inform. Theory* **2019**, 65, 3724–3737.
- 482 27. Schwartz, M.; Vardy, A. On the stopping distance and the stopping redundancy of codes. *IEEE Trans. Inform. Theory* **2006**, 52, 922–932.
- 483 28. Bocharova, I.E. Weight enumerators of high-rate convolutional codes based on the Hamming code. *Problemy Peredachi Informatsii* **1991**, 27, 86–91.
- 484 29. Bocharova, I.E.; Kudryashov, B.D.; Skachek, V.; Yakimenka, Y. Distance Properties of Short LDPC Codes and their Impact on the BP, ML and Near-ML Decoding Performance. International Castle Meeting on Coding Theory and Applications. Springer, 2017, pp. 48–61.
- 485 30. Sadeghi, P.; Kennedy, R.A.; Rapajic, P.B.; Shams, R. Finite-state Markov modeling of fading channels. – A survey of principles and applications. *IEEE Signal Processing Magazine* **2008**, 25, 57–80.
- 486 494

495 © 2019 by the authors. Submitted to *Journal Not Specified* for possible open access  
496 publication under the terms and conditions of the Creative Commons Attribution (CC BY) license  
497 (<http://creativecommons.org/licenses/by/4.0/>).